NeuroImage: Clinical 31 (2021) 102741

Contents lists available at ScienceDirect

NeuroImage: Clinical

journal homepage: www.elsevier.com/locate/ynicl

Blood-brain barrier dysfunction significantly correlates with serum matrix metalloproteinase-7 (MMP-7) following traumatic brain injury

Paul Nichols [a,*], Javier Urriola [b,c], Stephanie Miller [d], Tracey Bjorkman [d], Kate Mahady [e], Viktor Vegh [h,i], Fatima Nasrallah [b], Craig Winter [a,f,g]

[a] Department of Neurosurgery, Royal Brisbane and Women's Hospital, Australia
[b] Queensland Brain Institute, The University of Queensland, Australia
[c] Australian e-Health Research Centre, CSIRO, Brisbane, Australia
[d] University of Queensland Centre for Clinical Research, The University of Queensland, Royal Brisbane and Women's Hospital, Australia
[e] Department of Radiology, Royal Brisbane and Women's Hospital, Australia
[f] Faculty of Medicine, The University of Queensland, Australia
[g] School of Clinical Sciences, Queensland University of Technology, Australia
[h] The Centre for Advanced Imaging, The University of Queensland, Australia
[i] The ARC Centre for Innovation in Biomedical Imaging Technology, Brisbane, Australia

ARTICLE INFO

Keywords:
Traumatic brain injury
Blood brain barrier
Matrix metalloproteinase
Dynamic contrast enhanced magnetic resonance imaging
K^{Trans}

ABSTRACT

Objectives: To determine if radiological evidence of blood brain barrier (BBB) dysfunction, measured using Dynamic Contrast Enhanced MRI (DCE-MRI), correlates with serum matrix metalloproteinase (MMP) levels in traumatic brain injury (TBI) patients, and thereby, identify a potential biomarker for BBB dysfunction.

Patients and Methods: 20 patients with a mild, moderate, or severe TBI underwent a DCE-MRI scan and BBB dysfunction was interpreted from K^{Trans}. K^{Trans} is a measure of capillary permeability that reflects the efflux of gadolinium contrast into the extra-cellar space. The serum samples were concurrently collected and later analysed for MMP-1, −2, −7, −9, and −10 levels using an ELISA assay. Statistical correlations between MMP levels and the K^{Trans} value were calculated. Multiple testing was corrected using the Benjamin–Hochberg method to control the false-discovery rate (FDR).

Results: Serum MMP-1 values ranged from 1.5 to 49.6 ng/ml (12 ± 12.7), MMP-2 values from 58.3 to 174.1 ng/ml (109.5 ± 26.7), MMP-7 from 1.5 to 31.5 ng/mL (10 ± 7.4), MMP-9 from 128.6 to 1917.5 ng/ml (647.7 ± 749.6) and MMP-10 from 0.1 to 0.6 ng/mL (0.3 ± 0.2). Non-parametric Spearman correlation analysis on the data showed significant positive relationship between K^{Trans} and MMP-7 ($r = 0.55$, $p < 0.01$). Correlations were also found between K^{Trans} and MMP-1 ($r = 0.74$, $p < 0.0002$) and MMP-2 ($r = 0.5$, $p < 0.025$) but the actual MMP values were not above reference ranges, limiting the interpretation of results. Statistically significant correlations between K^{Trans} and either MMP-9 or −10 were not found.

Conclusion: This is the first study to show a correlation between DCE measures and MMP values in patients with a TBI. Our results support the suggestion that serum MMP-7 may be considered as a peripheral biomarker quantifying BBB dysfunction in TBI patients.

1. Introduction

Traumatic brain injury (TBI) represents a significant health and socioeconomic problem worldwide. The Australian Institute of Health and Welfare estimate the prevalence of TBI to be 107 per 100,000 people and in the US an estimated 1.7 million civilians sustain a TBI each year (Fortune and Wen, 1999). Patient outcome relates to both the primary structural brain injury and the development of secondary molecular mechanisms that cause subsequent damage, such as hypoxia–ischemia, neuroinflammation, lipid peroxidation, glutamate excitotoxicity, and blood–brain barrier (BBB) disruption (Sahuquillo et al.). The anatomical substrates of the BBB are comprised of endothelial cells, which are held

* Corresponding author: Department of Neurosurgery, Level 7. Ned Hanlon Building, Royal Brisbane and Women's Hospital. Butterfield Road, Herston, QLD 4029, Australia.
E-mail address: paul.nichols@health.qld.gov.au (P. Nichols).

https://doi.org/10.1016/j.nicl.2021.102741
Received 23 February 2021; Received in revised form 20 May 2021; Accepted 21 June 2021
Available online 24 June 2021

together by tight junctions, with associated astrocytes that limit the paracellular flux of solutes (Cucullo et al., 2011). Functionally this has an essential role in regulating the interstitial fluid microenvironment such that any compromise may lead to alterations in extracellular ion concentrations, neuronal disruption, increased vasogenic oedema, and raised intracranial pressure (Chow and Gu, 2015).

Both immediate and delayed dysfunction of the BBB have been observed in TBI and the hypothesis that BBB damage is an important factor in determining post-injury progression and patient outcome is increasingly emphasized (Neuwelt et al., 2008). The ability to measure the severity of BBB impairment following TBI could potentially aid in both patient outcome prognostication and in the current management of head injury patients. Defining a severely altered BBB in the setting of a head injury may, for example, modify fluid and blood pressure parameters so as not to worsen *peri*-contusional vasogenic oedema. The identification of on-going BBB processes, either harmful or reparative, that are potentially contributory to poor recovery from a seemingly mild TBI is also becoming increasingly important. Additionally, quantifying the extent of BBB damage may aid the validation of novel therapeutic drugs trialled to repair blood–brain barrier dysfunction. There is no current standard for the assessment of BBB dysfunction and further investigation into the identification of a potential peripheral biomarker is warranted (Thrippleton et al., 2019). A peripheral biomarker that is well correlated with a validated radiological measure of BBB dysfunction would have significant practical implications in the ongoing management and assessment of BBB dysfunction. It could allow for the diagnosis and monitoring of BBB dysfunction without the need for dedicated MRI assessment.

Dynamic contrast-enhanced magnetic resonance imaging (DCE-MRI) has previously been used to evaluate the extent of BBB dysfunction in brain tumours, ischemia, neuroinflammatory disorders, and trauma (Armitage et al., 2011; Cha, 2006; Zhang et al., 2014). It has been one of the main in-vivo research imaging methods utilised for the investigation of the extent of BBB dysfunction by measuring K^{Trans} (i.e. the volume transfer constant), the quantitative parameter extracted from DCE-MRI data. A damaged BBB enables the extravasation of low molecular weight intravenous contrast agents and the accumulation in the extravascular cellular space leads to both increased longitudinal relaxation rates and signal intensity in T1 weighted images. DCE-MRI utilises this T1 enhancement to detect and calculate indices related to the absorption and excretion of the MRI contrast medium. This is expressed as K^{Trans}, which reflects the number of contrast agent molecules delivered to the interstitial space per unit time (Tofts et al., 1999). Wei et al. (Wei et al., 2011) found significant differences in early K^{Trans} values between severe and moderate vs. mild TBI in experimental animal models of TBI. Lu et al. (Lu et al., 2018) later confirmed a sustained increase in K^{Trans} value in a controlled cortical injury.

The role of MMPs in TBI-induced BBB disruption has been a growing area of investigation in recent years (Planas et al., 2001). They are calcium-dependant zinc endopeptidases of the metzincin superfamily (Stöcker et al., 1995) and with the exception of MMP-28, are ubiquitously expressed in mammalian organisms. There are currently 24 human MMP homologues described and they are categorised into subfamilies such as gelatinases (MMPs −2 and −9), collagenases (MMPs −1, −8 and −13) and endopeptidases (MMP-7). They have a role in morphogenesis, cell migration and angiogenesis and are also involved in pathophysiological processes such as wound healing, inflammation and cancer (Rempe et al., 2016).

MMPs have a significant role in the regulation of the extracellular matrix (ECM) (Loffek et al., 2011) and they likely affect BBB integrity in head injuries by digesting and remodelling the ECM surrounding brain capillaries and by degrading tight junction proteins that seal the endothelium (Lischper et al., 2010; Feng et al., 2011). The composition of the BBB basement membrane includes Type IV collagen, laminin and fibronectin (Chakraborti et al., 2003); all of which are known to be degraded by MMPs. Additionally, MMPs directly compromise vascular integrity resulting in BBB dysfunction (Rempe et al., 2016). To further explore the role of MMP levels, we hypothesised that blood MMP levels would correlate with the degree of BBB permeability as measured using K^{Trans} in patients with TBI.

This study sought to address whether MMPs measured in serum blood correlated with DCE-MRI measured BBB dysfunction to determine if MMPs could act as a biomarker of BBB dysfunction in TBI. A serum biomarker would have great practical implications in the diagnosis and monitoring of BBB dysfunction, particularly in centres where access to MRI is limited or not practical. It would also have potential research implications in monitoring response to novel treatment strategies.

2. Materials and methods

2.1. Study subjects and design

The study was approved by the local Human Research and Ethics Committee (HREC/16/QRBW/604). TBI patients admitted to the Neurosurgical unit at the Royal Brisbane and Women's Hospital were approached for enrolment into the study. Inclusion criteria were patients aged between 18 and 80 with a radiologically verified TBI. Consent was gained from the patient or the next of kin. Exclusion criteria included patients with significant multi-trauma, known neurodegenerative diseases or significant mental health disorders and when the MRI was contraindicated (e.g. contrast allergy).

For each patient, details of age and initial Glasgow Coma Score (GCS) were collected (Table 1). The predominant finding on the CT brain scan was documented, i.e., diffuse axonal injury, contusion, traumatic subarachnoid haemorrhage or extra-axial haematoma and the head injury classified into mild (GCS 13–15), moderate (GCS 9–12) or severe (GCS 3–8) (Teasdale and Jennett, 1974).

2.2. Magnetic resonance imaging protocols

All images were obtained using a 3 T MRI scanner (Prisma, Siemens Healthcare, Germany) using a 32-channel head array coil. The MRI protocols consisted of an anatomical T1-weighted Magnetisation Prepared Rapid Gradient-Echo (MPRAGE) scan acquired with the following parameters: TE = 2.26 ms, TR = 1900, FA = 9 degrees, Acquisition matrix = 256 × 256, with 1 mm^3 isotropic voxel. The dynamic contrast-enhanced MRI (DCE-MRI) acquisition was performed using a 3D gradient-echo (GRE) T1-weighted Controlled Aliasing in Parallel Imaging Results in Higher Acceleration-volumetric interpolated breath-hold examination sequence (CAIPIRINHA-VIBE) (TE = 1.8 ms, TR = 4.35 ms, FA = 9 degrees, Acquisition matrix 221 × 200, resolution 0.94 × 0.94 × 0.9, number of measurements = 20, slices per volume = 208). Baseline images were acquired. Subsequently, during the first 2 min, and while the dynamic acquisition was continuing, the contrast agent Gadavist (GE Healthcare, USA) was injected as a bolus (0.1 mmol/kg) in to the antecubital vein. A total of 20 dynamic volumes were acquired with a temporal resolution of 55 s per volume. A post-contrast T1 MPRAGE was then obtained with the same parameters as the pre-contrast T1-weighted image.

2.3. MRI analysis and Pre-processing

Image pre-processing was performed using the FMRIB Software Library (FSL), Statistical Parametric Mapping (SPM12) and Matlab (MATLAB R2018b; The MathWorks, Inc., Natick, MA). DCE-MRI pre-processing steps included realignment of the volumes of the time-series to the first baseline volume, followed by tissue class segmentation and image bias field inhomogeneity correction using SPM12. For each patient, a visual inspection of all pre-processed DCE-MRI volumes and the realignment matrix was performed to detect volumes affected by motion artefacts, which were manually removed and replaced by a three-dimensional mean image from two adjacent volumes during the

Table 1
Clinical information, matrix metalloproteinases (MMP) and Dynamic Contrast-enhanced Magnetic Resonance Imaging (DCE-MRI) values of the 20 patients. (CHC: Contusional Haemorrhagic Core; GCS: Glasgow Coma Score; IQR: Interquartile range; TBI: Traumatic Brain Injury; >OOR: out-of-range i.e. values above the detectable threshold at 1:60 dilution, NAB: Normal Appearing Brain).

ID	Age	GCS category	GCS at scene	Days post injury	MMP1	MMP2	MMP7	MMP9	MMP10	CHC volume (mm3)	K^{Trans} CHC (min-1)	K^{Trans} NAB (min-1)	K^{Trans} ratio (CHC/NAB)
P01	52	Mild	14	5	18.8	100.5	11.0	589.9	0.19	811	0.027	0.000	61.8
P02	25	Mild	14	9	11.7	110.7	6.9	128.6	0.03	11,284	0.107	0.001	84.4
P03	66	Mild	14	8	49.6	138.9	31.5	142.2	0.33	1515	0.014	0.001	18.2
P04	35	Moderate	10	14	11.2	100.1	11.2	230.3	0.19	13,939	0.061	0.001	42.4
P05	19	Severe	7	18	6.3	129.8	8.9	1917.5	0.14	160	0.022	0.001	16.4
P06	23	Moderate	12	15	12.2	127.7	12.0	>OOR	0.69	14,768	0.039	0.000	108.4
P07	48	Moderate	12	15	7.3	129.5	11.4	496.9	0.67	1962	0.042	0.003	13.9
P08	26	Mild	15	4	5.4	88.2	4.9	201.7	0.17	989	0.058	0.002	27.3
P09	36	Severe	6	30	4.5	135.1	15.1	156.7	0.19	5798	0.021	0.001	35.3
P10	20	Mild	14	6	14.3	106.4	10.1	389.7	0.26	5887	0.026	0.002	16.5
P11	18	Moderate	10	20	27.3	115.9	10.5	>OOR	0.33	13,953	0.016	0.000	35.2
P12	20	Mild	15	4	8.4	112.3	13.9	699.4	0.64	922	0.002	0.000	5.8
P13	50	Mild	15	6	7.2	132.7	14.2	244.3	0.29	1209	0.035	0.003	13.8
P14	41	Mild	14	10	38.0	174.1	22.0	1270.2	0.46	21,470	0.055	0.001	58.7
P15	40	Mild	13	2	2.1	88.9	1.9	>OOR	0.37	854	0.003	0.001	2.3
P16	38	Mild	13	4	4.4	85.9	1.7	263.5	0.23	752	0.019	0.002	11.8
P17	23	Mild	13	3	1.6	91.4	1.5	358.8	0.63	5844	0.010	0.002	5.0
P18	22	Mild	13	1	1.5	86.8	2.2	2946.3	0.47	4217	0.007	0.002	2.9
P19	30	Mild	13	4	3.4	58.3	3.0	603.0	0.15	3214	0.015	0.003	5.2
P20	43	Mild	15	3	5.4	76.8	5.5	372.4	0.21	2651	0.008	0.001	9.3
Median	**33.8 (mean)**	–	**13.0**	**6.0**	**7.2**	**108.5**	**10.3**	**372.4**	**0.28**	**2932.5**	**0.0215**	**0.0014**	**16.4**
IQR	13.4 (SD)	–	2	10.3	8.2	40.9	8.0	372.7	0.27	6264	0.0273	0.0013	28.7

contrasted phase, producing a mean image of the pre-contrast DCE-MRI baseline. DCE-MRI images were resampled to 1 mm^3 isotropic resolution, and thus matching with the structural pre- and post-contrast T1-weighted images. Structural images were then rigidly registered to the first DCE volume using FSL flirt.

DCE-MRI image analysis was performed using the ROCKETSHIP toolbox (Barnes et al., 2015) running within MATLAB (R2018b). For each patient, the individual vascular input function (VIF) was extracted from the mean of three 1 mm^3 isotropic ROIs placed on the lumen of mid-cerebral arteries bilaterally and in the superior sagittal sinus of the pre-processed DCE-MRI volumes.

To obtain the whole-brain BBB permeability maps, the Patlak pharmacokinetic model was used (Patlak and Blasberg, 1985; Patlak et al., 1983). The model describes a highly perfused two-compartment tissue with unidirectional transport from blood plasma into the extra-vascular extracellular space (EES). Thus, the resulting BBB permeability maps, at a high spatial resolution, contained the K^{Trans} measurement on each voxel and was expressed in units of min^{-1}.

2.4. Region-of-interest selection and extraction

Three different masks were created to allow the study of the relationship between MMPs and pathological BBB permeability measurements. First, a *brain mask* of the pre-contrast T1-weighted image was obtained using antsBrainExtraction.sh (using the Open Access Series of Imaging Studies-OASIS template as tissue priors (Marcus et al., 2007) as implemented in the ANTs neuroimaging toolbox v.2.3.4. (Avants et al., 2009). A specialist neuroradiologist (KM) inspected each brain mask to ensure that the mask was an accurate reflection of the BBB region. From the same structural image, grey (GM) and white matter (WM) were segmented using SPM. The tissue probability maps in the native space were then thresholded at 0.95 and combined into a single GM-WM mask.

2.5. Contusional haemorrhagic-core (CHC) mask

This mask was aimed to delineate the haemorrhagic, contused brain parenchyma and vasogenic oedema lesion by depicting the central contusional region(s) of increased contrast enhancement following TBI. The mask was generated from the subtraction of the spatially registered structural post- and pre-contrast T1-weighted images. The GM-WM mask was used to estimate the threshold of the T1-difference image, set at mean plus two standard deviations. The threshold adjusted T1-difference image was then used as input for a semi-automatic segmentation method involving the filling of the contrast-enhancement injury lesion on successive iterations using region competition snakes as implemented in IKTsnap (ITK-SNAP v3.4, 2015). For this segmentation, 2 mm diameter spherical seeds were placed in non-vascular contusional regions of high signal intensity of the thresholded T1-difference image prior to running the segmentation algorithm. A neuroradiologist (KM), who had all structural and subtraction DCE images, inspected the semi-automatic results and adjusted any voxels accordingly.

2.6. Normal-appearing tissue mask and ratio with CHC

To compare the permeability values of the contrast-enhanced injury with the normal-appearing brain, a patient-specific normal appearing tissue mask was generated from the subtraction between the GM-WM mask and the Haemorrhagic core mask.

2.7. K^{Trans} ratio between contusional core and normal-appearing tissue mask.

It has been shown that in normal-appearing GM and WM, the K^{Trans} value is low but not zero (Larsson et al., 2009; Cramer et al., 2014; Barnes et al., 2016). Systematic noise in the measurement, motion, small amount of leakage of contrast-enhanced Gd through the intact BBB and normal aging (Montagne et al., 2015) has been identified to influence normal permeability measures. To account for normal-BBB variability's, the ratio between the mean K^{Trans} value of the CHC and the mean normal-appearing tissue mask was used to quantify the degree of BBB leakiness of the TBI lesion relative to the GM and WM parenchyma. The mean was obtained from non-zero voxels using the FSL command fslstats -M on each respective 1 mm isotropic masks. Thus, patients with higher K^{Trans} ratio reflect an increased permeability of the contusional core compared to the permeability of normal-appearing tissue.

3. Blood sampling and processing

Blood samples were collected in EDTA collection tubes on the same day as the MRI scan. Ten ml of blood was centrifuged at 1600 × *g* for 10 min, the sera extracted and stored at −80 degreesC and later analysed using a multiplex immunoassay (HMMP2MAG-55 K, Merck Millipore, Australia). Serum samples were diluted to 1:20, 1:30 or 1:60 where results were out of range. All samples were performed in duplicate; the mean fluorescence intensity was used to calculate MMP values. MMPs −1, −2, −7, −9, and −10 values were obtained.

4. Statistical analysis

GraphPad Prism 9 (GraphPad Software, Inc., San Diego, California, USA) was used for statistical analysis. The Shapiro-Wilk normality test was used to determine the distribution of the variables. The test showed that GCS, MMP and DCE-MRI values did not follow a Gaussian distribution (See Appendix table A1), hence the Mann-Whitney U and Kruskal-Wallis test were used to compare group differences, and the Spearman's rank correlation was used to assess the relationship between non-normally distributed variables. The significance alpha level was set to $p < 0.05$. To adjust for multiple testing, the Benjamini–Hochberg method was used to control the false-discovery rate (FDR) with a significance level set at $p < 0.05$ (Benjamini and Hochberg, 1995) (See Appendix A2).

5. Results

5.1. Patient demographics

A total of 20 patients completed the study (18 males, 2 females) with an age range of 18–66 years. Of these, mechanisms of injury included falls, assaults, and motor vehicle accidents. The patients were classified into mild (n = 14), moderate (n = 4), and severe (n = 2) using the GCS score (Teasdale and Jennett, 1974). The predominant CT finding was multiple contusions followed by acute subdural haematoma and traumatic subarachnoid haemorrhage.

5.2. DCE-MRI: Results and K^{Trans} findings

The DCE-MRI results are shown in Table 1. The median contusional haemorrhagic core (CHC) was 2933 mm^3 (IQR: 939–9935) with a median K^{Trans} value of 0.0215 min^{-1} (IQR: 0.011–0.041). This compares to a K^{Trans} value of 0.0014 min^{-1} (IQR: 0.001–0.003) for normal-appearing tissue. When we compared the CHC permeability measures between different head injury groups we found no statistical differences in the

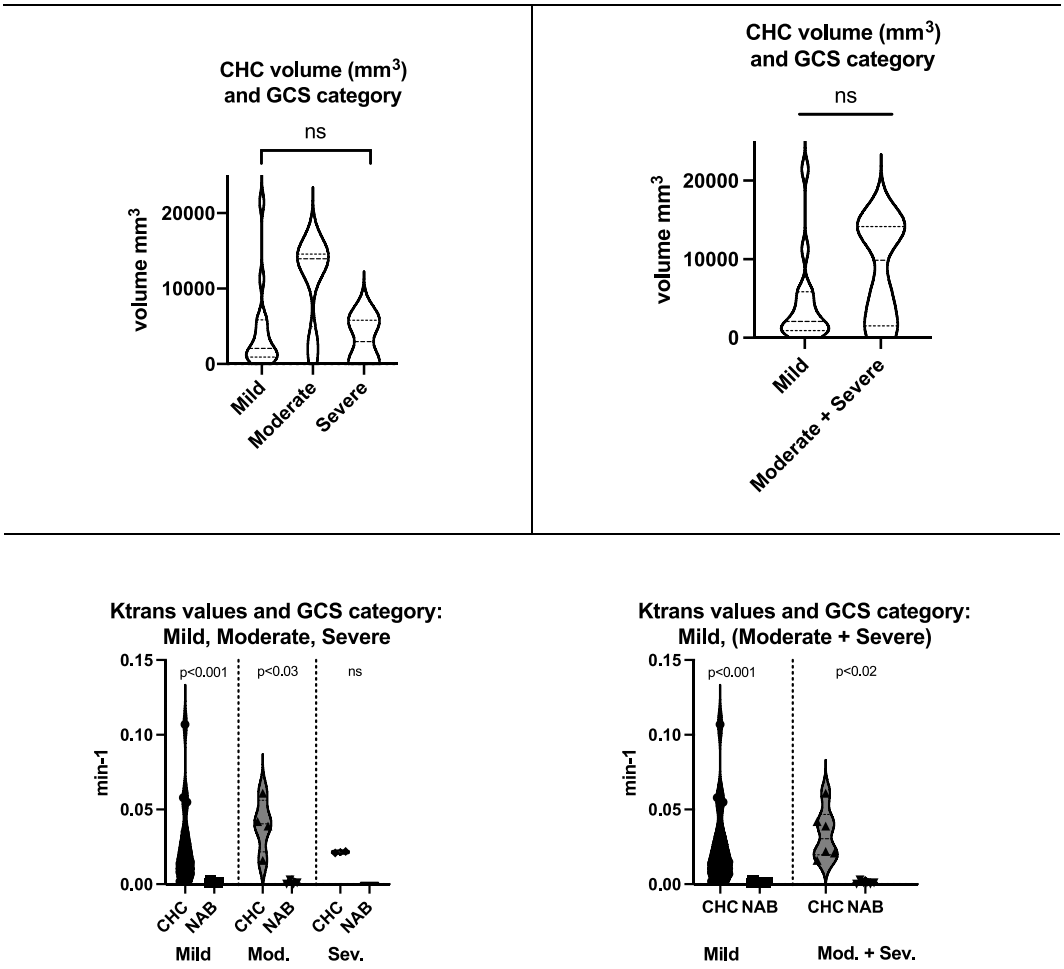

Fig. 1. Glasgow Coma Scale (GCS) category and contusional haemorrhagic core (CHC) DCE-MRI values. Top row: No differences between the volume of the CHC. Bottom left : K^{Trans} CHC and normal-appearing brain (NAB) across three GCS categories. Bottom right: K^{Trans} CHC and normal-appearing brain (NAB) when combining moderate and severe GCS category in the same group.

volume or K^{Trans} values (Kruskal–Wallis test -See Fig. 1). K^{Trans} values were increased in the CHC region when compared to the rest of the brain for both mild and moderate patient groups ($p < 0.001$ and $p < 0.03$ FDR corrected, respectively). Due to the small dataset of severe TBI patients ($n = 2$), no differences were detected between CHC and normal-appearing brain in the two severe head injuries. When merging the severe and moderate TBI group the K^{Trans} values within the CHC were also increased ($p < 0.02$) (See Fig. 2). The median K^{Trans} ratio between CHC and normal-appearing brain was 16.4 (8.43 – 37.1 interquartile range (IQR). Fig. 2 displays representative images for two illustrative patients.

5.3. Serum matrix metalloproteinases

Serum MMP-1 values ranged from 1.5 to 49.6 ng/ml (12 ± 12.7), MMP-2 values from 58.3 to 174.1 ng/ml (109.5 ± 26.7), MMP-7 from 1.5 to 31.5 ng/mL (10 ± 7.4), MMP-9 from 128.6 to 1917.5 ng/ml (647.7 ± 749.6) and MMP-10 from 0.1 to 0.6 ng/mL (0.3 ± 0.2). MMP-7 and MMP-9 were elevated compared to the literature (Dimitrova et al., 2019; Vočka et al., 2019) with MMP-9 values out of range (despite a 1:60 dilution) for three patients. The serum levels of MMP-1, −2 and −10 levels were within the limits of published normal ranges.

5.4. Correlations between MMP serum levels and DCE-MRI

Fig. 3 provides the correlations and Spearman's coefficients (r) and p-values ($p < 0.05$ FDR corrected) calculated between the MMP concentrations and the permeability ratio between CHC and normal-appearing tissue. We found a significant correlation between K^{Trans} ratios and MMP-7 ($p < 0.01$). Correlations were also found between K^{Trans} and MMP-1 ($p < 0.0002$) and MMP-2 ($p < 0.025$) but the MMP values were not above reference ranges. No correlations were seen with K^{Trans} and either MMP-9 or −10.

6. Discussion

This work is the first to demonstrate a significant correlation between DCE measures of BBB leakiness and serum MMP levels following TBI. We confirm elevated serum MMP-7 levels above published reference ranges and a statistically significant correlation with the K^{Trans} ratio between abnormal and intact BBB regions ($p < 0.01$, FDR corrected). The K^{Trans} ratio also correlated with serum levels of MMP-1 and MMP2, although serum MMP-1, and −2 levels were not elevated compared to typically normal blood levels. Our MMP-7 levels ranged from 1.5 to 31.5

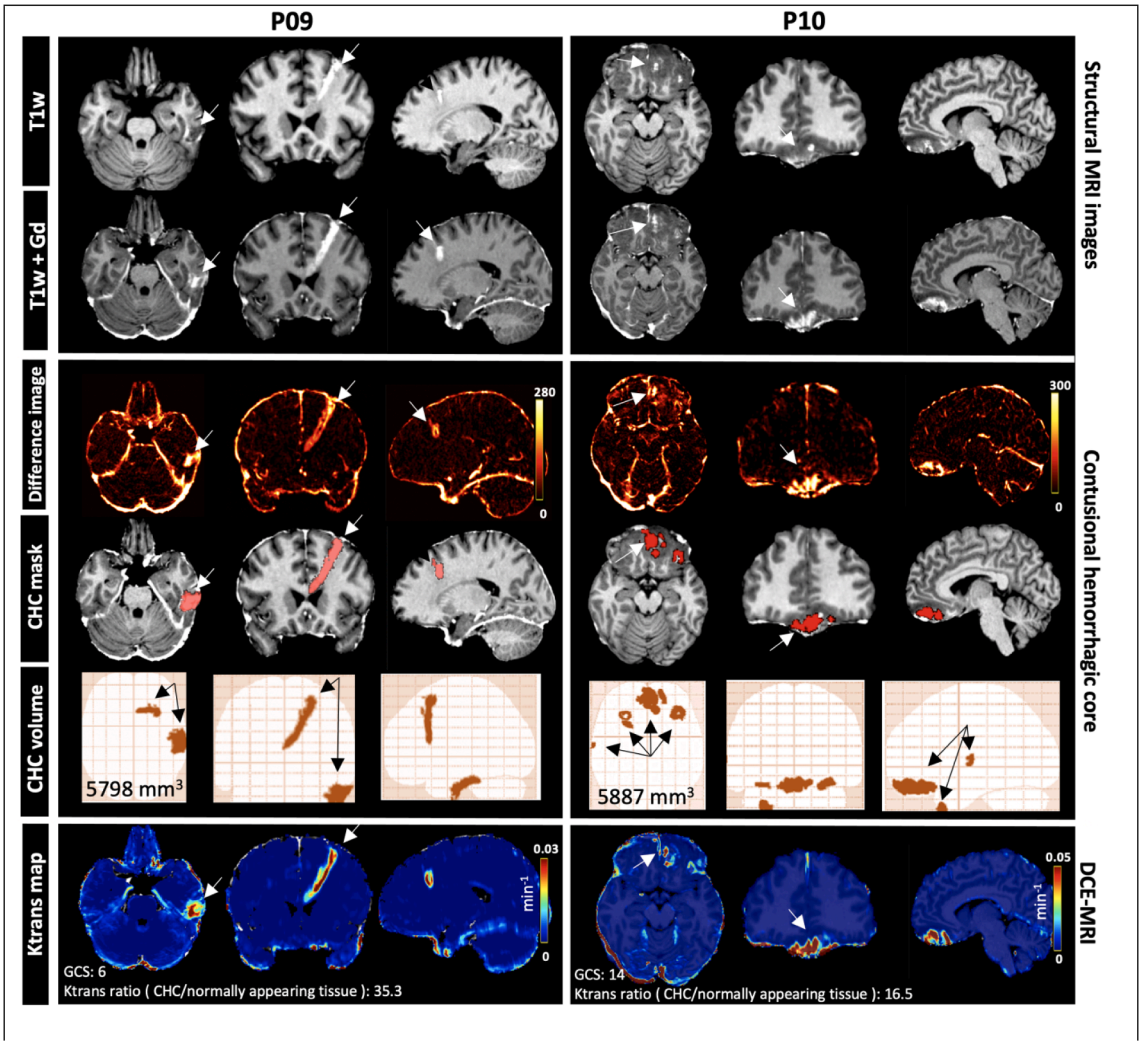

Fig. 2. Examples of a patient with severe (P09) and mild TBI (P10). The top two rows correspond to the registered T1 pre (first row) and post (second row) contrast-enhanced MPRAGE volumes of each patient and the white arrows define the contusional haemorrhagic core. T1-difference image and contusional haemorrhagic core mask are shown in rows three and four with the total mask volume of the haemorrhagic lesion overlayed on the glass brain (row 5). Row 6 represents the whole brain K^{Trans} illustrating the regions of increased BBB permeability in a blue to red color-coded scale. The GCS and the respective K^{Trans} ratio are shown between the values of the haemorrhagic lesion and normal-appearing tissue masks. CHC: contusional haemorrhagic core; Gd: Gadolinium-contrast; GCS: Glasgow Coma Score. (For interpretation of the references to color in this figure legend, the reader is referred to the web version of this article.)

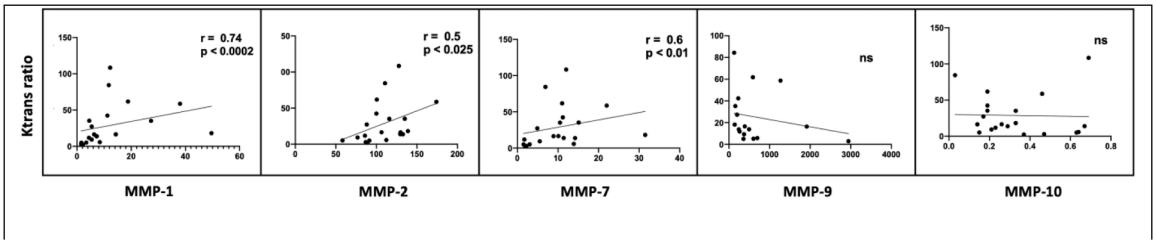

Fig. 3. Scatter plot showing the Spearman correlation (r) and p-value ($p < 0.05$ FDR corrected) of each Matrix Metalloproteinases (ng/ml) against the K^{Trans} ratio.

ng/mL (10 ± 7.4) compared to the reference ranges quoted in the literature of 1.48 ± 0.09 ng/mL and 3.38 ± 0.09 ng/mL (Dimitrova et al., 2019; Vočka et al., 2019). While this represents a broad range, when we compare our results to these historical ranges, 75% (n = 15) of our cohort showed elevated MMP-7 levels and this included all the severe and moderate TBI patients (n = 6) and 64% (n = 9) of the mild head injuries.

DCE-MRI is an *in vivo* imaging method used for quantification of the severity of BBB dysfunction by measuring the coefficient K^{Trans}. Indeed, this DCE-MRI measure has been shown to reflect severity-dependent changes in permeability in a quantitative fashion (Wei et al., 2011). A previous study, also using DCE-MRI to measure BBB compromise in head injured patients reported a tendency for K^{Trans} to increase with the severity of TBI, but the trend was not statistically significant (Winter et al., 2015). In our study we found the median K^{Trans} value for the contusional haemorrhagic core was 0.0215 min^{-1} (IQR: 0.011–0.041) compared to the normal-appearing brain tissue with a value of 0.0014 min^{-1} (IQR: 0.001–0.003). We used the ratio of the mean K^{Trans} between the contusional core and normal-appearing tissue, as opposed to direct readings of K^{Trans}, to minimise the contribution of noise, motion, physiological leakage, and aging (Larsson et al., 2009; Cramer et al., 2014; Barnes et al., 2016; Montagne et al., 2015) and found that the ratio significantly correlates with MMP levels.

The role of MMPs in BBB compromise has been a point of discussion in many reviews and studies (Rempe et al., 2016; Seo et al., 2012). Specifically, MMP-7 is a zinc and calcium-dependent endopeptidase that has a direct role in the integrity of the BBB, degrading a range of ECM substrates (including type IV collagen). It has been found to be elevated in other brain pathologies with BBB compromise such as multiple sclerosis and brain tumours (Dimitrova et al., 2019; Pardo and Selman, 2005; Elkington et al., 2011). A recent paper by Castellazi et al (Castellazzi et al., 2018) analysed CSF MMP-7 levels and noted elevated levels in patients with longer disease duration, in keeping with our increased MMP-7 levels measured up to a maximum of 30 days post-injury. MMP-7 is able to cleave the tight junction protein VE-cadherin, disrupting the BBB, and a hallmark of the structural manifestations of MS is the presence of MRI lesions confirming BBB damage. Metalloproteinase inhibitors have even been trialled in the treatment of MS (Khokha et al., 2013). The possible ubiquitous nature of MMP-7 in brain injury is further supported by its implication in HIV dementia (Parks et al., 2004); the authors describing an association between MMP-7 levels and brain atrophy. Recent work by Soderhohm et al. (Söderholm et al., 2018) suggests that MMP-7 may also be more important in the risk of spontaneous subarachnoid haemorrhage in the general population, compared to MMP-2 and −9, which were previously thought to have a strong association, again citing ECM degradation as potentially causal.

MMP-7 is also extensively expressed in microglia (Ke et al., 2017) and has been shown to be integral in the development of neuroinflammatory lesions in animal models of MS (Experimental Autoimmune Encephalitis, EAE). Buhler et al. (Buhler et al., 2009) confirms that MMP-7 may act by reducing BBB integrity, facilitating the influx of immune-competent cells and thereby fuelling inflammation. Furthermore, Guilfoyle et al (Guilfoyle et al., 2015) confirmed elevated MMP-7 levels in *peri*-contusional brain using microdialysis but reported no difference between damaged and normal brain during five-days following a severe brain injury. Although another dialysis study (Roberts et al., 2013) confirmed a late upsurge in MMP-7 levels (up to 6.5 days post injury), the results are not directly comparable to those presented here given the shorter time interval post-injury, the TBI patient cohort being predominantly severe and the use of cerebral microdialysis samples. Although an accurate characterisation of the exact role of MMP-7 in the brain is not entirely evident, its detection in multiple pathologies would suggest an integral role in BBB degradation. We add to this hypothesis by correlating the level with K^{Trans}, a structural measure of BBB integrity, and suggest serum MMP-7 level may provide an accurate biomarker for TBI induced BBB damage.

In line with previous research we are able to confirm elevated serum MMP-9 levels in TBI patients though a significant correlation with BBB dysfunction was not found. MMP-9 levels ranged from 128.6 to 1917.5 ng/ml (647.7 ± 749.6) with three values out of range (despite a 1:60 dilution) compared to historical ranges of 45.7–233.6 ng/ml (Cossins et al., 1997) and 30–357 ng/ml (Nikkola et al., 2005; Riedel et al., 2000). Raised MMP-9 levels following severe TBI have been documented in the CSF (Grossetete et al., 2009) and ECF in microdialysis studies (Vilalta et al., 2008). Guilfoyle et al (Guilfoyle et al., 2015) confirmed an initial rise in the dialysate MMP-9 levels within the first 24 h in *peri*-contusional brain but this was followed by a decline.

Our serum MMP-1 values ranged from 1.5 to 49.6 ng/ml (12 ± 12.7) and MMP-2 values from 58.3 to 174.1 ng/ml (109.5 ± 26.7). Surprisingly, correlations were found between K^{Trans} ratio and MMP-1 ($p < 0.0002$) and MMP-2 ($p < 0.025$) despite serum MMP values were not above reference ranges. MMP-1 is known to act on type I, II and III collagen in the ECM and is involved in the cleavage of a number of non-matrix substrates and cell surface molecules (Pardo and Selman, 2005) and could therefore be considered as a potential indicator of on-going BBB compromise. The literature confirms variability in the expression of MMP-2 following head injury. Viliata et al. (Vilalta et al., 2008) confirmed an acute increase in MMP-2 reducing after 24 h. Conversely, the study by Roberts el al. (Roberts et al., 2013) described an initially low concentration MMP-2 concentration, followed by a 48-hour peak, and then a progressive decline. It has additionally been proposed that MMP-2 may only be elevated in a subset of patients with TBI (Guilfoyle et al., 2015). The combination of variable post-TBI expression, short-lived elevation and in our study a lack of elevation above normal ranges would indicate that MMP-1 and MMP-2 cannot be realistically considered as potential BBB biomarkers. MMP-10 levels were not elevated above the normal range and no statistical correlation with K^{Trans} was found. MMP-10, also known as stromelysin-2, is expressed in epithelial cells and macrophages (Zhang et al., 2014; McMahan et al., 2016) but its physiological function remains unclear. Further study is needed to identify its role in TBI.

The Patlak model has been shown to be highly sensitive to assess the BBB permeability with high spatial resolution and brain coverage, allowing to quantify subtle BBB leakage (Heye et al., 2016). Hence, a possibility is that the normal MMP-1 and MMP-2 levels correspond to levels taken outside of the respective MMP peak. It will be relevant to analyse the temporal dynamic and relationship between MMP and BBB

dysfunction. However, our study has two limitations that prevent the interpretation of a subset of our data for this purpose. (1) The number of participants on the entire cohort was 20 and splitting the data into small and large TBI – DCE MRI temporal intervals will reduce the power of the study to find associations between the variables, and (2) the data of the subjects included in this study was not optimised to investigate the effect of the time interval between TBI and DCE-MRI as this factor was not part of the experimental design. Future studies scanning patients at different temporal intervals will be needed to assess if MMP-1 and MMP-2 have earlier or later temporal window than MMP-7.

We acknowledge that our conclusions are based on a limited number of patients and this inherently limits the robustness of our analyses. Further studies involving a greater number of participants with serial DCE-MRI scans, coupled with concurrent serum values, would lead to a greater understanding of the temporal profile of MMP expression. Additionally, biomarkers such as S100B and GFAP have been well studied in the literature, they were found to be potentially lacking in their applicability to function as a clinical biomarker. Our study design could serve as a template for further study in the field of BBB dysfunction. As further potential biomarkers become apparent it would be possible to use this design to quantify their value with correlation to DCE-MRI.

In our group, due to logistical reasons, patients were scanned at different days post-TBI. The MRI was delayed for the severe TBI patients until they had been extubated because of safety concerns around transport of an intubated intensive care patient, or for the moderate TBI patients who were too agitated for an acute MRI. The number of days post head injury that the DCE-MRI scan was performed ranged from 3 to 30 (9.2 $\pm$ 7.4) and we would suggest that this does not invalidate the premise that MMP-7 may be suitable as a BBB biomarker. BBB dysfunction relates to the initial primary brain injury but it also develops in a delayed time course secondary to neuro-inflammation and metabolic disturbances after even a mild TBI, such that any delayed correlation between BBB dysfunction and MMP-7 is valid. In recent times the investigation of the long-term sequelae of mild TBI and the development of Chronic Traumatic Encephalopthy (CTE) is taking centre stage such that a marker providing insight into a potentially important delayed secondary process, such as BBB dysfunction, should be welcomed.

7. Conclusion

We suggest that serum MMP-7 may be considered as a peripheral biomarker quantifying BBB dysfunction within the contusional core of traumatic brain injuries as measured by K^{Trans} from DCE-MRI data. To our knowledge, a direct correlation between measures of DCE-MRI and MMP serum levels has not been reported previously. A larger cohort of patients may strengthen the association and provide more insights into the role of MMP-7, and MMPs in general, in BBB dysfunction.

Funding

This work was supported by The Motor Accident Insurance Commission (MAIC), The Queensland Government, Australia [Grant number 2014000857].

CRediT authorship contribution statement

Paul Nichols: Methodology, Investigation, Project administration, Writing - original draft. **Javier Urriola:** Formal analysis, Writing - original draft. **Stephanie Miller:** Investigation. **Tracey Bjorkman:** Investigation. **Kate Mahady:** Formal analysis. **Viktor Vegh:** Writing - review & editing. **Fatima Nasrallah:** Conceptualization, Methodology, Funding acquisition, Supervision, Writing - review & editing. **Craig Winter:** Supervision, Writing - review & editing.

Declaration of Competing Interest

The authors declare that they have no known competing financial interests or personal relationships that could have appeared to influence the work reported in this paper.

Appendix A. Supplementary data

Supplementary data to this article can be found online at https://doi.org/10.1016/j.nicl.2021.102741.

References

Fortune, N., Wen, X. The definition, incidence and prevalence of acquired brain injury in Australia. Australian Institute of Health and Welfare. AIHW Cat no DIS 15 Canberra: AIHW 1999.

Sahuquillo, J., Poca, M., Amoros, S. Current aspects of pathophysiology and cell dysfunction after severe head injury. Curr. Pharm. Des. 7, 1475-1503. doi10.2174/1381612013397311.

Cucullo, L., Hossain, M., Puvenna, V., Marchi, N., Janigro, D., 2011. The role of shear stress in Blood-Brain Barrier endothelial physiology. BMC Neurosci. 12 (1) https://doi.org/10.1186/1471-2202-12-40.

Chow, B.W., Gu, C., 2015. The molecular constituents of the blood-brain barrier. Trends Neurosci. 38 (10), 598–608. https://doi.org/10.1016/j.tins.2015.08.003.

Neuwelt, E., Abbott, N.J., Abrey, L., Banks, W.A., Blakley, B., Davis, T., Engelhardt, B., Grammas, P., Nedergaard, M., Nutt, J., Pardridge, W., Rosenberg, G.A., Smith, Q., Drewes, L.R., 2008. Strategies to advance translational research into brain barriers. Lancet Neurol. 7 (1), 84–96. https://doi.org/10.1016/S1474-4422(07)70326-5.

Thrippleton, M.J., Backes, W.H., Sourbron, S., Ingrisch, M., van Osch, M.J.P., Dichgans, M., Fazekas, F., Ropele, S., Frayne, R., van Oostenbrugge, R.J., Smith, E.E., Wardlaw, J.M., 2019. Quantifying blood-brain barrier leakage in small vessel disease: Review and consensus recommendations. Alzheimer's Dementia. 15 (6), 840–858. https://doi.org/10.1016/j.jalz.2019.01.013.

Armitage, P.A., Farrall, A.J., Carpenter, T.K., Doubal, F.N., Wardlaw, J.M., 2011. Use of dynamic contrast-enhanced MRI to measure subtle blood–brain barrier abnormalities. Magn. Reson. Imaging 29 (3), 305–314. https://doi.org/10.1016/j.mri.2010.09.002.

Cha, S., 2006. Update on brain tumor imaging: from anatomy to physiology. Am. J. Neuroradiol. 27 (3), 475–487.

Zhang, X., Quan, X., Lu, S., Huang, F., Yang, J., Chan, Q., Lin, T., 2014. The clinical value of dynamic contrast-enhanced magnetic resonance imaging at 3.0T to detect prostate cancer. J. Int. Med. Res. 42 (5), 1077–1084. https://doi.org/10.1177/0300060514541827.

Tofts, P.S., Brix, G., Buckley, D.L., et al., 1999. Estimating kinetic parameters from dynamic contrast-enhanced T(1)-weighted MRI of a diffusable tracer: standardized quantities and symbols. J. Magn. Reson. ImagingJMRI. 10 (3), 223–232. https://doi.org/10.1002/(sici)1522-2586(199909)10:3<223:aid-jmri2>3.0.co;2-s.

Wei, X.-E., Wang, D., Li, M.-H., Zhang, Y.-Z., Li, Y.-H., Li, W.-B., 2011. A useful tool for the initial assessment of blood-brain barrier permeability after traumatic brain injury in rabbits: dynamic contrast-enhanced magnetic resonance imaging. The J. Trauma: Injury Infect. Critical Care 71 (6), 1645–1651. https://doi.org/10.1097/TA.0b013e31823498eb.

Lu, L., Wang, M., Wei, X., Li, W., 2018. 20-HETE inhibition by HET0016 decreases the blood-brain barrier permeability and brain edema after traumatic brain injury. Front. Aging Neurosci. 10 https://doi.org/10.3389/fnagi.2018.00207.

Planas, A.M., Solé, S., Justicia, C., 2001. Expression and activation of matrix metalloproteinase-2 and -9 in rat brain after transient focal cerebral ischemia. Neurobiol. Dis. 8 (5), 834–846. https://doi.org/10.1006/nbdi.2001.0435.

Stöcker, W., Grams, F., Reinemer, P., Bode, W., Baumann, U., Gomis-Rüth, F.-X., Mckay, D.B., 1995. The metzincins - Topological and sequential relations between the astacins, adamalysins, serralysins, and matrixins (collagenases) define a super family of zinc-peptidases. Protein Sci. 4 (5), 823–840. https://doi.org/10.1002/pro.v4:510.1002/pro.5560040502.

Rempe, R.G., Hartz, A.M.S., Bauer, B., 2016. Matrix metalloproteinases in the brain and blood-brain barrier: versatile breakers and makers. J. Cerebral Blood Flow Metabol. Official J. Int. Soc. Cerebral Blood Flow Metabol. 36 (9), 1481–1507. https://doi.org/10.1177/0271678X16655551.

Loffek, S., Schilling, O., Franzke, C.-W., 2011. Biological role of matrix metalloproteinases: a critical balance. Eur. Respir. J. 38 (1), 191–208. https://doi.org/10.1183/09031936.00146510.

Lischper, M., Beuck, S., Thanabalasundaram, G., Pieper, C., Galla, H.-J., 2010. Metalloproteinase mediated occludin cleavage in the cerebral microcapillary endothelium under pathological conditions. Brain Res. 1326, 114–127. https://doi.org/10.1016/j.brainres.2010.02.054.

Feng S, Cen J, Huang Y, et al. Matrix metalloproteinase-2 and -9 Secreted by Leukemic Cells Increase the Permeability of Blood-Brain Barrier by Disrupting Tight Junction Proteins. Avraham HK, ed. PLoS One. 2011;6(8):e20599. doi:10.1371/journal.pone.0020599.

Chakraborti, S., Mandal, M., Das, S., et al., 2003. Regulation of matrix metalloproteinases: an overview. Mol. Cell. Biochem. 253 (1/2), 269–285. https://doi.org/10.1023/a:1026028303196.

Teasdale, G., Jennett, B., 1974. Assessment of coma and impaired consciousness. Lancet 304 (7872), 81–84. https://doi.org/10.1016/s0140-6736(74)91639-0.
Barnes, S.R., Ng, T.S.C., Santa-Maria, N., Montagne, A., Zlokovic, B.V., Jacobs, R.E., 2015. ROCKETSHIP: a flexible and modular software tool for the planning, processing and analysis of dynamic MRI studies. BMC Med. Imaging 15 (1). https://doi.org/10.1186/s12880-015-0062-3.
Patlak, C.S., Blasberg, R.G., 1985. Graphical evaluation of blood-to-brain transfer constants from multiple-time uptake data. Generalizations. J. Cereb. Blood Flow Metab. 5 (4), 584–590. https://doi.org/10.1038/jcbfm.1985.87.
Patlak, C.S., Blasberg, R.G., Fenstermacher, J.D., 1983. Graphical evaluation of blood-to-brain transfer constants from multiple-time uptake data. J. Cereb. Blood Flow Metab. 3 (1), 1–7. https://doi.org/10.1038/jcbfm.1983.1.
Marcus, D.S., Wang, T.H., Parker, J., Csernansky, J.G., Morris, J.C., Buckner, R.L., 2007. Open Access Series of Imaging Studies (OASIS): cross-sectional MRI data in young, middle aged, nondemented, and demented older adults. J. Cogn. Neurosci. 19 (9), 1498–1507. https://doi.org/10.1162/jocn.2007.19.9.1498.
Avants, B.B., Tustison, N., Song, G., 2009. Advanced normalization tools (ANTS). Insight J. 2 (365), 1–35.
Larsson, H.B.W., Courivaud, F., Rostrup, E., Hansen, et al, Measurement of brain perfusion, blood volume, and blood brain barrier permeability, using dynamic contrast enhanced T1-weighted MRI at 3 tesla. Magn Reson Med. 2009;62(5):1270-1281. doi.org10.1002mrm.22136.
Cramer, S.P., Simonsen, H., Frederiksen, J.L., Rostrup, E., Larsson, H.B.W., 2014. Abnormal blood-brain barrier permeability in normal appearing white matter in multiple sclerosis investigated by MRI. Neuroimage Clin. 4, 182–189. https://doi.org/10.1016/j.nicl.2013.12.001.
Barnes, S.R, Ng, T.S., Montagne, A., et al. (2016). Optima acquisition and modeling parameters for accurate assessment of low KTrans blood-brain barrier permeability using dynamic contrast-enhanced MRI. Magn Reson Med. May;75(5):1967-77. doi: 10.1002mrm.25793.
Montagne, A., Barnes, S.R., Sweeney, M.D., Halliday, M.R., Sagare, A.P., Zhao, Z., Toga, A.W., Jacobs, R.E., Liu, C.Y., Amezcua, L., Harrington, M.G., Chui, H.C., Law, M., Zlokovic, B.V., 2015. Blood brain barrier breakdown in the aging human hippocampus. J. Neuron. 85 (2), 296–302. https://doi.org/10.1016/j.neuron.2014.12.032.
Benjamini, Y., Hochberg, Y., 1995. Controlling the false discovery rate: a practical and powerful approach to multiple testing. J. Roy. Stat. Soc.: Ser. B (Methodol.) 57 (1), 289–300.
Dimitrova, I., Tacheva, T., Mindov, I., Petrov, B., Aleksandrova, E., Valkanov, S., Gulubova, M., Vlaykova, T., 2019. Serum levels of MMP-7 in primary brain cancers and brain metastases. Biotechnol. Biotechnol. Equip. 33 (1), 881–885. https://doi.org/10.1080/13102818.2019.1626282.
Vočka, M., Langer, D., Fryba, V., Petrtyl, J., Hanus, T., Kalousova, M., Zima, T., Petruzelka, L., 2019. Serum levels of TIMP-1 and MMP-7 as potential biomarkers in patients with metastatic colorectal cancer. Int. J. Biol. Mark. 34 (3), 292–301. https://doi.org/10.1177/1724600819866202.
Winter, C., Bell, C., Whyte, T., et al., 2015. Blood-brain barrier dysfunction following traumatic brain injury: correlation of K (trans) (DCE-MRI) and SUVR (99mTc-DTPA SPECT) but not serum S100B. Neurol. Res. 37 (7), 599–606. https://doi.org/10.1179/1743132815Y.000000001.
Seo, J.H., Guo, S., Lok, J., et al., 2012. Neurovascular matrix metalloproteinases and the blood brain barrier. Curr. Pharm. Des. 18 (25), 3645–3648. https://doi.org/10.2174/13816121802002742.
Pardo, A., Selman, M., 2005. MMP-1: the elder of the family. Int. J. Biochem. Cell Biol. 37 (2), 283–288. https://doi.org/10.1016/j.biocel.2004.06.017.
Elkington, P., Shiomi, T., Breen, R., et al. (2011). MMP-1 drives immunopathology in human tuberculosis and transgenic mice. J. Clin. Invest. 121(5) 1827-1833. doi: 10.1172/JCI45666. Epub 2011 Apr 25. PMID: 21519144; PMCID: PMC3083790.
Castellazzi, M., Ligi, D., Contaldi, E., Quartana, D., Fonderico, M., Borgatti, L., Bellini, T., Trentini, A., Granieri, E., Fainardi, E., Mannello, F., Pugliatti, M., 2018. Multiplex matrix metalloproteinases analysis in the cerebrospinal fluid reveals potential specific patterns in multiple sclerosis patients. Front. Neurol. 9 https://doi.org/10.3389/fneur.2018.01080.
Khokha, R., Murthy, A., Weiss, A., 2013. Metalloproteinases and their natural inhibitors in inflammation and immunity. Nat. Rev. Immunol. 13 (9), 649–665. https://doi.org/10.1038/nri3499. PMID: 23969736.
Parks, W.C., Wilson, C.L., López-Boado, Y.S., 2004. Matrix metalloproteinases as modulators of inflammation and innate immunity. Nat. Rev. Immunol. 4 (8), 617–629. https://doi.org/10.1038/nri1418. PMID: 15286728.
Söderholm, M., Nordin, F., Nilsson, J., Engström, G., 2018. High serum level of matrix metalloproteinase-7 is associated with increased risk of spontaneous subarachnoid haemorrhage. Stroke 49 (7), 1626–1631. https://doi.org/10.1161/STROKEAHA.118.020660. Epub 2018 Jun 7 PMID: 29880550.
Ke, B., Fan, C., Yang, L., Fang, X., 2017. Matrix metalloproteinases-7 and kidney Fibrosis. Front. Physiol. 8 https://doi.org/10.3389/fphys.2017.00021.
Buhler, L.A., Samara, R., Guzman, E., Wilson, C.L., Krizanac-Bengez, L., Janigro, D., Ethell, D.W., 2009. Matrix metalloproteinase-7 facilitates immune access to the CNS in experimental autoimmune encephalomyelitis. BMC Neurosci. 10 (1), 17. https://doi.org/10.1186/1471-2202-10-17.
Guilfoyle, M.R., Carpenter, K.L.H., Helmy, A., Pickard, J.D., Menon, D.K., Hutchinson, P. J.A., 2015. Matrix metalloproteinase expression in contusional traumatic brain injury: a paired microdialysis study. J. Neurotrauma 32 (20), 1553–1559. https://doi.org/10.1089/neu.2014.3764.
Roberts, D.J., Jenne, C.N., Léger, C., Kramer, A.H., Gallagher, C.N., Todd, S., Parney, I.F., Doig, C.J., Yong, V.W., Kubes, P., Zygun, D.A., 2013. Association between the cerebral inflammatory and matrix metalloproteinase responses after severe traumatic brain injury in humans. J. Neurotrauma 30 (20), 1727–1736. https://doi.org/10.1089/neu.2012.2842.
Cossins, J.A., Clements, J.M., Ford, J., Miller, K.M., Pigott, R., Vos, W., Van Der Valk, P., De Groot, C.J.A., 1997. Enhanced expression of MMP-7 and MMP-9 in demyelinating multiple sclerosis lesions. Acta Neuropathol. 94 (6), 590–598.
Nikkola, J., Vihinen, P., Vuoristo, M., Kellokumpu-Lehtinen, P., Kähäri, V.-M., Pyrhönen, S., 2005. High serum levels of matrix metalloproteinase-9 and matrix metalloproteinase-1 are associated with rapid progression in patients with metastatic melanoma. Clin. Cancer Res. 11 (14), 5158–5166. https://doi.org/10.1158/1078-0432.CCR-04-2478.
Riedel, F., Götte, K., Schwalb, J., et al. Serum levels of matrix metalloproteinase 2 and 9 in patients with head and neck squamous cell carcinoma. Anticancer Res. 2000 Sep-Oct;20(5A):3045-3049.
Grossetete, M., Phelps, J., Arko, L., Yonas, H., Rosenberg, G.A., 2009. Elevation of matrix metalloproteinases 3 and 9 in cerebrospinal fluid and blood in patients with severe traumatic brain injury. Neurosurgery 65 (4), 702–708. https://doi.org/10.1227/01.NEU.0000351768.11363.48.
Vilalta, A., Sahuquillo, J., Poca, M.A., et al., 2008. Brain contusions induce a strong local overexpression of MMP-9. Results of a pilot study. Acta neurochirurgica Supplement. 102, 415–419. https://doi.org/10.1007/978-3-211-85578-2_81.
Zhang, G., Miyake, M., Lawton, A. et al. (2014). Matrix metalloproteinase-10 promotes tumor progression through regulation of angiogenic and apoptotic pathways in cervical tumors. BMC Cancer 14, 310. doi.org/10.1186/1471-2407-14-310.
McMahan, R., Birkland, T., Smigiel, K., et al., 2016. Stromelysin-2 (MMP10) moderates inflammation by controlling macrophage activation. J. Immunol. 197 (3), 899–909. https://doi.org/10.4049/jimmuol.1600502.
Heye, A.K., Thrippleton, M.J., Armitage, P.A., Valdés Hernández, M.C., Makin, S.D., Glatz, A., Sakka, E., Wardlaw, J.M., 2016. Tracer kinetic modelling for DCE-MRI quantification of subtle blood-brain barrier permeability. Neuroimage 125, 446–455. https://doi.org/10.1016/j.neuroimage.2015.10.018.